Endovascular Electrical Stimulation - A Novel Hemorrhage Control Technique

*Noa Kezurer [1,2†], Eitan Heldenberg [3†], Nairouz Farah [1, 2†], Nadav Ivzan [1, 2], Yossi Mandel [*1, 2]*

***Abstract*— *Objective:* In this study we present a novel approach for inducing vasoconstriction by pulsed electrical treatment delivered via endovascular electrodes, which can be used in cases where external access to the vessel is limited. *Methods:* Using computer simulations, we optimized various geometries of endovascular electrodes to maximize the induced electric field on the arterial wall. Using the optimal configuration parameters, we investigated endovascular induced vasoconstriction in both the carotid and femoral sheep arteries. *Results:* Endovascular electrodes induced robust vasoconstriction in the carotid artery of sheep, showing gradual recovery following treatment. Moreover, the obtained vasoconstriction was accompanied by a sevenfold decrease in blood loss for 100% constriction, compared with no treatment (6ml vs 42ml, $p<0.001$). The femoral artery was less amenable to the electrical treatment, which we hypothesize results from the reduced density of the sympathetic system's innervation of the adventitia of the sheep femoral artery, as was validated by immunohistochemical analysis. Finally, treatment safety was validated through arterial histological studies, in which no adverse effect was observed, and through computer modeling, which depicted a negligible temperature increase. *Significance:* These results are an important step toward developing a novel approach for inducing reversible and controlled vasoconstriction in arteries that are remote from access.**

Index Terms- Vasoconstriction, endovascular, hemorrhage control, vascular surgery.

This paper was supported by a grant from the Israeli Ministry of Science and Technology (YM).

1) School of Optometry and Vision Science, Faculty of Life Sciences, Bar-Ilan University, Ramat-Gan, Israel
2) Bar Ilan's Institute for Nanotechnology and Advanced Materials (BINA), Bar Ilan University. Ramat-Gan, Israel
3) Department of Vascular Surgery, Assaf Harofeh Medical Center, Israel
†equal contribution
* corresponding author: Dr. Yossi Mandel at yossi.mandel@biu.ac.il.

I. Introduction

Traumatic injury of blood vessels with bleeding is the leading cause of death among individuals younger than 40 years of age in the US, with hemorrhagic shock accounting for 30-40 percent of traumatic mortality[1]. Furthermore, uncontrolled bleeding is the most common preventable cause of death on a battlefield[2]. In both military and civilian settings, a major challenge is the effective treatment of uncontrolled bleeding resulting from non-compressible hemorrhage in difficult-to-access vessels, where tourniquets cannot be used, such as cases of junctional bleeding (e.g., femoral artery bleeding) or internal bleeding in solid organs (e.g., spleen and liver). Although various techniques have been introduced for controlling hemorrhage on site before reaching the hospital [3]–[6], none are optimal. Moreover, even in a hospital setting, controlling arterial hemorrhage is challenging, in both elective (e.g., the arterial bypass procedure) and emergency (e.g., traumatic vessel repair) scenarios, since the surgeon must extensively expose the vessel and mechanically clamp both the proximal and distal sides of the artery. This procedure is relatively complex and obviously can only be performed by a highly trained vascular surgeon. The rising need and the aforementioned limitations of available techniques for controlling non-compressible hemorrhage or for use in elective vascular surgery have generated great interest in developing new techniques for eliciting vasoconstriction and hemorrhage control.

In previous publications we have demonstrated that short electrical pulses delivered by extravascular electrodes elicit robust and controlled vasoconstriction in the femoral and mesenteric arteries of rats [7], [8]. Specifically, in these reports we demonstrated that control of bleeding, caused by complete resection of the femoral artery and vein [7] or following a traumatic liver injury in rats or rabbits[9], can be achieved by pulsed electrical treatment. We hypothesize that the obtained vasoconstriction is induced by the combined activation of sympathetic nerves innervating blood vessels and the direct activation of the vessels' smooth muscle[10].

In the above-mentioned studies, electrical stimulation was delivered via extravascular electrodes in experimental settings, where blood vessels can be easily exposed. However, in most traumatic cases, and in some elective surgical procedures an endovascular electrode approach is more advantageous, enabling easy and quick access for the delivery of a pulsed electric field treatment to the injured blood vessel via an intact remote vessel while eliminating the need for prolonged exposure of the diseased or injured vessel. Moreover, this approach provides access to the distal side of the vessel, thus eliminating retrograde blood flow and enabling better hemostasis control.

Here we introduce a novel approach based on the endovascular application of electrical pulses for vasoconstriction induction, and we present a comprehensive study performed on a large animal model (the sheep carotid artery, Fig. 1a,b). Our results show a robust vasoconstriction response to a pulsed electric field in the carotid artery of a large animal model (sheep), which increased with the pulse voltage amplitude, and recovered gradually. More importantly, electrically induced vasoconstriction was accompanied by a sevenfold reduction in blood loss from an injured carotid artery, compared with a non-

treated artery. The close proximity between the electrodes and the heat-conducting blood flow prevent a significant increase in temperature during treatment; as was estimated by computer simulation. Finally, histological examination revealed no apparent injury to the treated arteries and validated our hypothesis of the possible involvement of the sympathetic innervation in the induced vasoconstriction. Our results indicate that endovascular electrically pulsed vasoconstriction is an effective and safe procedure and call for future studies to further evaluate the potential of this novel approach for controlling vasoconstriction in large arterial vessels as well as for possible clinical applications.

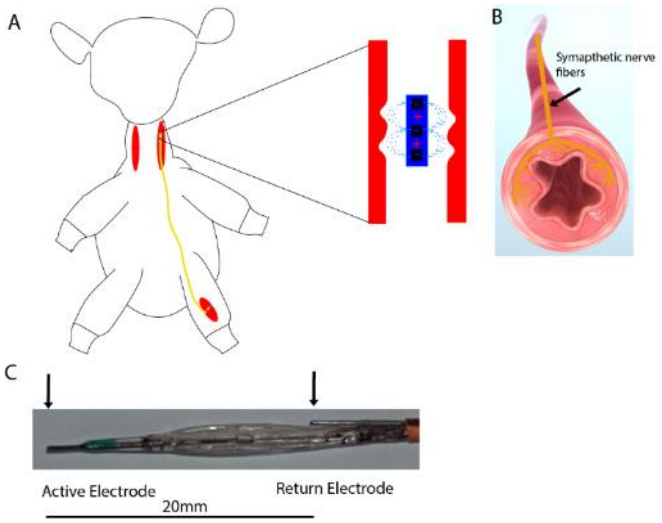

Figure 1. Endovascular vasoconstriction concept illustration. (A) Bipolar electrode introduced via the femoral artery to the carotid during a standard catheterization procedure. Blow up: the electrical field distribution induced by the bipolar configuration with the predicted two-site vasoconstriction. (B) An illustration of the postulated underlying mechanism, depicting an innervated constricted blood vessel. (C) An image of a bipolar electrode fabricated from medical guide wires of 0.035 mm diameter, 130 cm long (PT^{2TM}, light support; Boston Scientific), with a conductive core (either nitinol or stainless steel), and an insulating coating.

II. METHODS

A. Computer Simulations – general considerations.

Computer modelling was performed to investigate the distribution of the electric field induced by the currents endovascularly applied in a sheep carotid artery. As a first step, the sheep carotid artery was modelled as a 2D, 250 mm-long rectangle domain, with a diameter of 4.5 mm and a total thickness of 0.5 mm, incorporating different vessel wall layers (the intima, media, and adventitia)[11]. This domain was surrounded by a large rectangle representing the muscle and surrounding tissue (200 and 800 mm for the bipolar and monopolar configurations, respectively, which are described in the following sections). The electrical properties of the blood vessel and surrounding muscle were taken from an online database[12] based on the work of Gabriel et al. [13] and are summarized in Table I, whereas the electrical properties of each of the vessel wall layers were taken from[14],[15] and adapted to a stationary model. The thermal properties of the tissue were taken from the literature[9], [12], [16], [17] ,[18] and from the online database of the Foundation for Research on Information Technologies in Society[19](Table I).

The efficacy of inducing vasoconstriction was investigated for bipolar and monopolar electrode configurations. In the bipolar configuration the return electrode was in proximity to the active electrode, whereas in the monopolar configuration the return electrode was positioned on the outer boundary of the geometrical model, mimicking a large skin electrode, routinely used in electro surgical procedures[20]–[22]. The modeled electrodes' material was set to 304 stainless steel, similar to that used in the animal experiment described in the following section; their electrical and thermal properties are shown in Table I.

TABLE I
ELECTRICAL AND THERMAL PROPERTIES OF THE TISSUE

		Blood	*Adventitia*	*Media*	*Intima*	*Muscle*	*Electrode*
$\sigma(s/m)$	*Electrical Conductivity*	0.7	0.8	0.4	0.6	0.25	22x10^6
ε_r	*Relative permittivity*	1.4x10^4	1x10^7	1x10^7	1x10^7	1.4x10^7	1
ρ (kg/m^3)	*Density*	1000	1102	1102	1102	1090	7900
K(W/m*K)	*Thermal conductivity*	0.52	0.46	0.46	0.46	0.4	14
Cp(J/Kg*K)	*Heat Capacity*	3640	3306	3306	3306	3421	14
T(K)	*Temperature*	310.15	310.15	310.15	310.15	310.15	310.15
W(1/s)	*Perfusion rate*	184.95				0.017	
$\rho_m (W/m^3)$	*Metabolism rate*	33800					

B. Computer Simulation – Electric Field.

The electrical properties of the sheep carotid artery were simulated using COMSOL Multiphysics 5.2 with MATLAB R2013b, similarly to our previous reports [7],[21]. Using the parameters described in Table 1, each of the various blood vessel wall layers (e.g., intima, media, and adventitia) was modeled as a distinct characteristic domain.

The electrical potential and electric field for each spatial point in the model were calculated using COMSOL's electrical current physics model by solving the electric field equation:

$$\nabla(\sigma \nabla\emptyset) = 0 \qquad (1)$$

where σ is the electrical conductivity and $\emptyset$ is the potential at a specific location. The outer boundaries of the model were set to an insulating condition in which

$$-n * J = 0 \qquad (2)$$

where n represents the unit's outward normal vector and J represents the current density; a continuity condition was applied to all other boundaries.

The electric field distribution was calculated for a steady-state solution for an applied potential of 50V for both electrode configurations using a direct linear solver (MUMPS). For each configuration, the electric field in each point on the geometry was calculated, followed by averaging of the electric field inside the vessel wall, with the latter calculation used for inter-electrode distance optimization in the bipolar configuration.

The optimal inter-electrode distance of the bipolar configuration was reached at by running computer simulations in which the distance between the return and active electrode was changed, similarly to our previous publication[23]. Briefly, for each selected inter electrode distance, we analyzed the average arterial wall electric field amplitude and evaluated the field homogeneity by calculating the standard deviation of the electric field along the arterial wall across the entire width. The optimal distance was then defined as the distance at which the field average amplitude and the homogeneity reached a maximum.

C. Computer Simulation – the bioheat model

After the field equation was solved, the tissue temperature rise during electrical stimulation was estimated, similarly to our previous reports[7],[9] using the Joule heating (p)

$$p = \sigma|\nabla\emptyset|\text{^}2 \qquad (3)$$

where σ is the electrical conductivity and $\emptyset$ is the induced electrical potential.

The Joule heat generated during the treatment was then inserted as the heat source in the Pennes bioheat equation[24].

$$\rho c_p \frac{\partial T}{\partial t} = \nabla(k\nabla T) + w_b\, \rho_b c_b (T_a - T) + q''' + p \qquad (4)$$

where k is the thermal conductivity of the tissue, T is the temperature, $w_{b\_}$ is the blood perfusion, c_b is the heat capacity of the blood, T_a is the arterial temperature, q''' is the metabolic heat generation, p is the electric heat generation, ρ is the tissue density, and c_p is the heat capacity of the tissue. A boundary condition of heat flux was assigned to the outer boundaries of the muscle, with a total heat flux of 0, simulating a steady-state situation. The initial temperature of the whole geometry was set to 37°C (310.15K). Simulations were then performed for a pulse amplitude of 400V, a pulse width of 1ms, and a repetition rate of either 2 or 10Hz, and a 4-minute session for each of the configurations.

To estimate the expected temperature rise resulting from the applied treatment, we performed the simulation for a number of flow rates, based on the baseline perfusion rate (184 1/s) corresponding to various constriction levels, namely: 100% (no constriction), 10%, and 1%.

D. Design and fabrication of endovascular electrodes

The electrodes were designed to allow for easy access through a large vessel (e.g., the femoral artery or vein) and to enable stimulation of remote blood vessels at the entire vasculature. We therefore opted to fabricate the electrodes from medical guide wires of 0.035 mm diameter, 130 cm long (PT^{2TM}, light support; Boston Scientific) with a conductive core (either nitinol or stainless steel), and an insulating coating (Fig 1c). The flexible tip was cut and the insulating layer of the wire was removed to expose the conducting core while creating a 2mm electrode. Complete electrical insulation in the distal part of the wire was achieved by inserting and gluing the wire into a 3mm diameter catheter (Passeo-18, Biotronix).

As mentioned in the computer simulation section, we fabricated both bipolar and monopolar electrodes. In the bipolar configuration, both active and return electrodes (2mm long) were positioned on the endovascular device and fabricated as described above. The inter-electrode distance was set to 20mm, according to the optimization study, which was described above (and is described in further detail in our previous report [23]). In the monopolar configuration, the 2mm-long active electrode was inserted endovascularly, and a large stainless-steel plate, which was placed with a conducting gel on the animal abdomen, served as a return electrode.

The active and the ground electrodes were then connected to a pulse generator (ECM 830, BTX) and to an oscilloscope (TDS 3012B, Tektronix) for the acquisition and monitoring of the actual voltage and current delivered by the endovascular device.

E. Animal experiments

All animal care and experiments were carried out in accordance with guidelines for the humane care of animals and were approved by the institutional research in animal ethics committee. Eight sheep (Ovis aries, local breed Asaf, 70 kg weight) were placed in a supine position and were monitored for heart rate, temperature, and blood oxygen saturation levels throughout the experiment. Animals were anesthetized with TELAZOL® (tiletamine HCl and zolazepam HCl) IV induction (5mg/kg), with maintenance of Isoflurane via tracheal tube (1-2%) and paralyzed with Tracium (atracurium besylate). The animals' core body temperature was maintained at 37°C by a heating pad and the blood pressure was monitored and kept constant by intravenous fluids.

This article has been accepted for publication in a future issue of this journal, but has not been fully edited. Content may change prior to final publication. Citation information: DOI 10.1109/TBME.2018.2883212, IEEE Transactions on Biomedical Engineering

F. Endovascular application of pulsed electrical treatment

The target blood vessel (carotid artery) was accessed by catheterization through the femoral artery using standard guide wires and catheters (0.18", 8Fr, respectively) under guidance of a fluoroscopic imaging system widely used for angiography (Siemens Healthcare). The pre-treatment vessel diameter was evaluated by angiography, performed by injecting contrast media (Iopromide 0.7g/ml- Ultravist®) and X-ray imaging of the vessel. The artery was then stimulated for 1 min, at a pulse duration of 1 millisecond, a pulse repetition rate of 2 Hz, with voltage amplitudes of 25, 50, 100, 200 and 400V. Next, the post-stimulation blood vessel diameter was angiographically evaluated immediately after stimulation at a frame rate of 15-30 frames per second and the treatment effect was evaluated by calculating the maximal vessel constriction percentage using RadiAnt DICOM Viewer software. The gradual recovery of the vessel was then evaluated by repeated imaging of up to 120 minutes post treatment and the results were fitted to an exponential function using the minimum mean square error estimate. Each data point consisted of 4-6 repetitions.

G. Measuring the effect of endovascular pulsed electrical treatment on blood loss

The effect of pulsed electrical treatment on bleeding was evaluated by a cut in a distal point in the carotid artery, leaving an open intra-arterial catheter, and letting the artery bleed for 15 seconds into a container. The blood loss was then evaluated by weighing the blood. The artery was then electrically stimulated as previously described, to obtain a 50% and 100% vasoconstriction, and bleeding was evaluated again. The animal's blood pressure was kept constant during the entire experiment.

H. Histology

After stimulation, the animals were euthanized, and the treated artery was dissected and immersed in 10% buffered formalin overnight. The tissue was then dehydrated with a graded series of ethanol concentrations, fixed in paraffin, sectioned (4µm-thick sections obtained using the Leica Bond III system -Leica Biosystems Newcastle Ltd, UK), and stained with hematoxylin and eosin (H&E). To validate our hypothesis of sympathetic system innervation being a possible underlying mechanism for the observed vasoconstriction, samples were further processed for the sympathetic system marker Tyrosine Hydroxylase. The process involved fixating the sample in 4% PFA for 48 hours, dehydration in ethanol, and embedding in paraffin. Fixated tissues were then pretreated with epitope-retrieval solutions (ER, Leica Biosystems Newcastle Ltd, UK) followed by 30 minutes incubation with anti-Tyrosine hydroylase antibody (MAB318, Millipore DE). The Leica Refine-HRP kit (Leica Biosystems Newcastle Ltd, UK) was used for detection and counterstaining with Hematoxylin.

III. RESULTS

A. Computer Modeling and electrode configuration optimization:

Computer modelling of the electric field distribution was performed in order to optimize the electrodes' configurations and to predict the electric field profile induced by the pulsed treatment. The detailed electrical properties of the blood vessel, the various vessel wall layers, and the surrounding tissue were based on values obtained from literature, as is described in the Methods section. As can be observed in Fig. 2a, the monopolar configuration (with the distant large remote ground) resulted in a single distinct peak in the electric field along the vessel wall whose location corresponded to the center of the active electrode. In the bipolar configuration, on the other hand, two clear peaks in the electric field distribution can be observed, corresponding to the active and return electrode locations (Fig.2b).

The optimal inter-electrode distance was reached at by maximizing the electric field amplitude at the vessel wall while increasing the field's homogeneity, as was evaluated by a low field normalized standard deviation (see Methods). As shown in Fig. 2c, a maximal average field amplitude and a minimal normalized standard deviation value are obtained for an inter-electrode distance of 20mm.

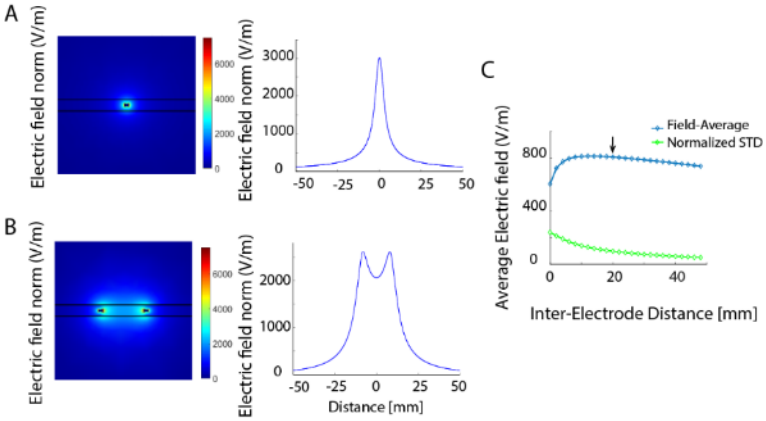

Figure 2. Electrical Field distribution. (A) The obtained electric field distribution for a monopolar configuration following a 50V pulse, at steady state (left). The electric field distribution along a cutline in the media layer of the blood vessel wall (Right). (B) The obtained electric field distribution for a bipolar configuration following a 50V pulse, at steady state (left). The electric field distribution along a cutline in the media layer of the blood vessel wall (Right). (C) The inter-electrode distance optimization process. The electric field average and the normalized standard deviation as a function of inter-electrode distance. Arrow: the optimal inter-electrode distance

B. Electrical pulses induce robust vasoconstriction in the sheep carotid artery

Following electrode configuration optimization, both monopolar and bipolar electrodes were fabricated from medical guide wires with a conducting core to allow for easy access through a large vessel (details are described in the Methods section). The animal (sheep) was anesthetized and the electrodes were introduced through the femoral artery toward the common carotid artery. Electrical pulses were then applied

This article has been accepted for publication in a future issue of this journal, but has not been fully edited. Content may change prior to final publication. Citation information: DOI 10.1109/TBME.2018.2883212, IEEE Transactions on Biomedical Engineering

and the response of the vessel to the applied treatment was studied using contrast-enhanced angiography acquired at 15 to 30 frames per second. The efficiency of the obtained constriction was then evaluated by estimating the change in the carotid artery diameter as observed from the angiography images, which reveal robust vasoconstriction in response to pulsed electrical treatment (Fig. 3, Suppl. Video 1 and 2). As predicted in our finite element model (Fig. 2a), the endovascular monopolar configuration resulted in a one-site constriction in the blood vessel (Fig. 3a,c,e), whereas the bipolar configuration resulted in a two-site constriction (Fig. 3b,d,f).

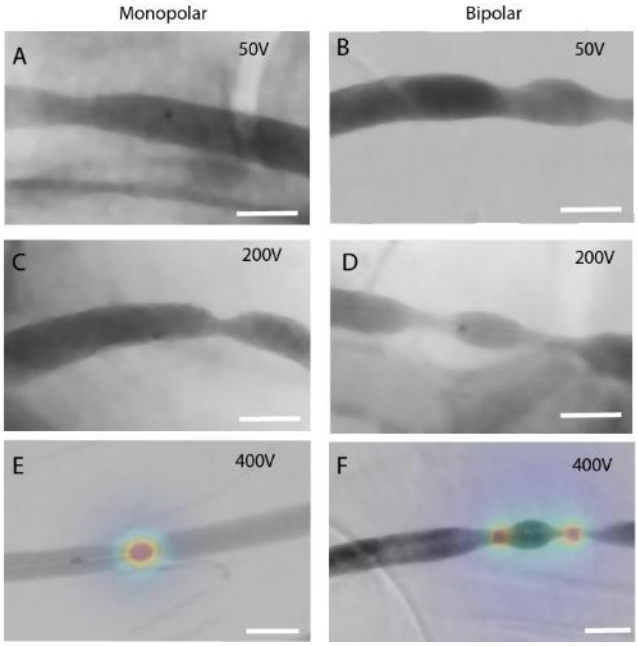

Figure 3. Angiogram images of the constricted carotid artery. (A), (C) Contrast-enhanced Angiogram images demonstrating the obtained vasoconstriction for the monopolar configuration induced by a 1msec pulse with increasing amplitudes of 50 and 200V (administered for 1min at a 2Hz repetition rate), resulting in 30% and 60% vasoconstriction, respectively. (B), (D) Contrast-enhanced angiogram images demonstrating the obtained vasoconstriction for the bipolar configuration induced by a 1msec pulse with increasing amplitudes of 50, 200V (administered for 1min at a 2Hz repetition rate) resulting in 30% and 75% vasoconstriction, respectively. (E) Obtained vasoconstriction in the monopolar configuration for a 400V, 1msec pulse applied for 1min at a 2Hz repetition rate, overlaid with a computer-simulated electric field demonstrating the good agreement between the obtained vasoconstriction and the predicted field distribution. (F)Obtained vasoconstriction in the bipolar configuration for a 400V, 1msec pulse applied for 1min at a 2Hz repetition rate, overlaid with a computer-simulated electrical field demonstrating the good agreement between the obtained vasoconstriction and the predicted field distribution. Scale bar - 1cm.

For both electrode configurations, the carotid artery vasoconstriction increased with pulse amplitude, almost reaching a plateau (of approximately 75%) at 400V with a 1ms pulse width at a repetition rate of 2Hz and a treatment duration of 1 min (Fig. 4a, b). The artery was completely constricted by a longer treatment of 4 minutes with the same pulse parameters (Fig. 4a,b, red circle), as clearly demonstrated in the angiography images, acquired after the prolonged treatment (Fig. 4c,d).

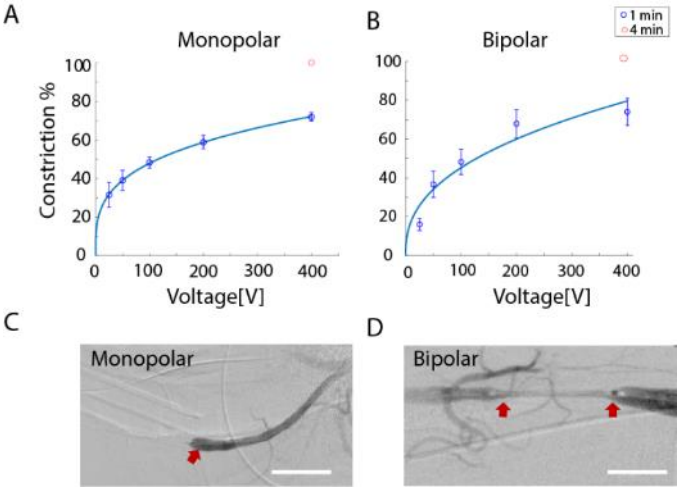

Figure 4. Vasocontraction as a function of pulse amplitude for the carotid artery. (A) The obtained vasoconstriction (constriction percentage from initial diameter) in the carotid artery for the monopolar configuration as a function of pulse amplitude (25-400V), for a pulse width of 1msec, administered for 1min at 2Hz (blue line) and 4min (red circle). (B) The obtained vasoconstriction in the carotid artery for the bipolar configuration as a function of pulse amplitude, for a pulse width of 1msec, administered for 1min at 2Hz (blue line) and 4min (red circle). (C) Complete vasoconstriction in the monopolar configuration following a 400V, 4min treatment session (1msec pulses, 2Hz repetition rate). (D) A complete vasoconstriction in the bipolar configuration following a 400V, 4min treatment session (1msec pulses, 2Hz repetition rate). Scale bar - 1cm.

Following the electrical treatment, the arterial diameter recovered gradually for the 100V- and the 200V-treated artery, almost fully recovering at 30 and 80 minutes post treatment, respectively, whereas for the 400V-treated artery, a significantly slower recovery was observed (as is inferred from the shorter exponential time constant of the fitting curves, as depicted in Fig. 5).

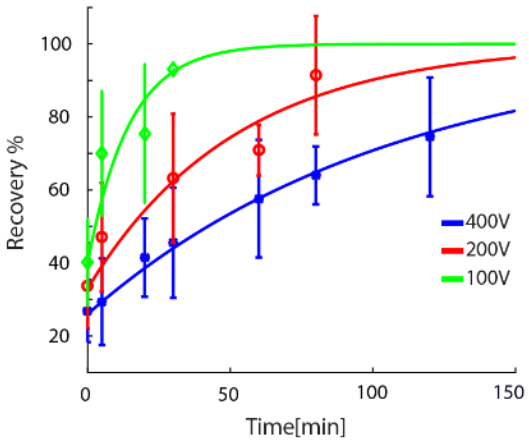

Figure 5. Recovery of the carotid artery following vasoconstriction. The observed recovery of the carotid artery following treatment with 1msec pulses administered for 1min at 2Hz for various amplitudes: 100V (green line), 200V (red line), and 400V (blue line), demonstrating the reversibility of the obtained vasoconstriction. Exponential time constants for the recovery fit curves were 7.3, 30 and 74 minutes for the 100, 200 and 400V, respectively.

This article has been accepted for publication in a future issue of this journal, but has not been fully edited. Content may change prior to final publication. Citation information: DOI 10.1109/TBME.2018.2883212, IEEE Transactions on Biomedical Engineering

C. Electrically induced vasoconstriction significantly reduces arterial blood loss

To assess the efficiency of the proposed method in controlling hemorrhage, we measured the amount of blood loss from an injured carotid artery over a 15-second episode following constriction of 50% and 100%, and compared the blood loss to no constriction (baseline). A sevenfold decrease in blood loss was observed for the 100% constricted artery, compared with no treatment (6ml vs 42ml, $p<0.001$), whereas 50% vasoconstriction yielded a moderate decrease in blood loss ($p=0.008$). These results highlight the efficacy of controlling blood loss through endovascular electrically induced vasoconstriction.

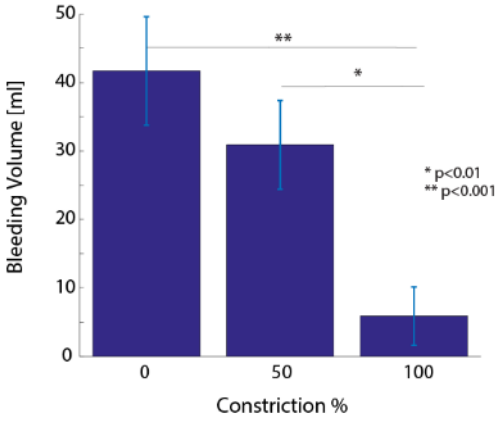

Figure 6. Bleeding control in the carotid artery. Bleeding control estimated by measuring the blood loss following vasoconstriction: 0% no treatment, 50% and 100% vasoconstriction. Significant differences in the bleeding volume were found when comparing no treatment to 100% constriction ($p<0.001$) and 50% to 100% ($p<0.01$).

D. The Bio-heat Model

In addition to electric field optimization, we used the computer-based simulations to estimate the temperature rise induced by the applied pulsed electrical treatment for a 400V pulse at pulse repetition rates of 2Hz and 10Hz (Fig. 7a,b). Since the blood flow rate is expected to significantly affect the temperature rise during treatment, the simulations were investigated at flow rates of 100%, 10%, and 1%. The maximal temperature rise on the arterial wall was negligible, but it increased with the decrease in flow rate and the increase in the repetition rate. For example, an increase of 0.65, 0.62, 0.61 °C was estimated for flow rates of 1%, 10%, and 100%, under the monopolar configuration for a 2Hz repetition rate and 400V amplitude, respectively (Fig. 7c). A similar negligible increase was observed for the same treatment parameters for the bipolar configuration. When a worst case-scenario of 1% for 400V pulses applied at 10Hz was investigated, a more significant temperature increase was observed (4°C), but it is still within safety limits[25](Fig. 7c). These results indicate that both configurations are safe even when administering a prolonged treatment, which significantly constricts the blood vessel.

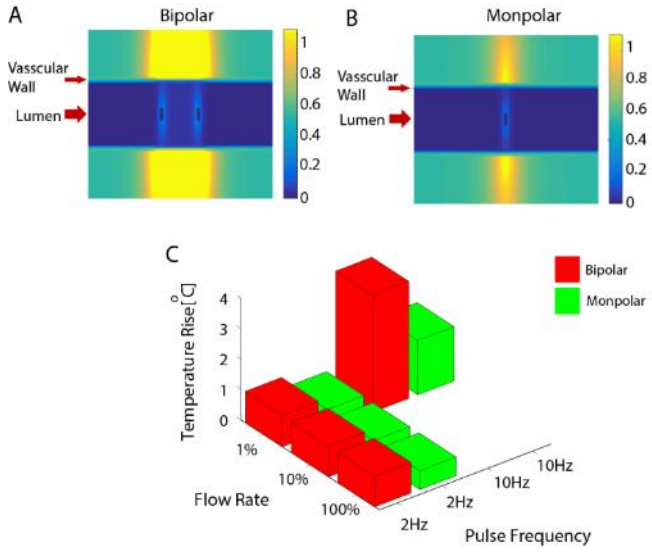

Figure 7. Temperature Simulations. (A) Estimated temperature increase profile following 1msec, 400V pulses administered for 4min at 2Hz for the bipolar configuration. The simulations where performed at a 1% flow rate. (B) Estimated temperature increase profile following 1msec, 400V pulses administered for 4min at 2Hz for the monopolar configuration. The simulations where performed at a 1% flow rate. (C) Maximal obtained temperature increase in the blood vessel wall as a function of flow rate for both electrode configurations (bipolar and monopolar) for pulses applied at either 2Hz or 10Hz (at the 1% flow rate).

E. Minimal constriction was observed in the femoral artery

Interestingly, in contrast to the robust constriction observed in the carotid artery, the femoral artery exhibited little to no constriction in response to electrical stimulation for both electrode configurations (Fig. 8a-c), even after a long treatment session of 4 min (Fig. 8c). We hypothesize that the different response to the applied treatment arises from the different innervations that these blood vessels receive from the sympathetic system, with the femoral artery being sparsely innervated, as is further demonstrated next.

F. Immunohistochemistry of blood vessels

Histological sections of the treated carotid artery revealed no significant pathological effects, compared with the control non-treated vessel, indicating the safety of the proposed method for vasoconstriction (Fig. 9).

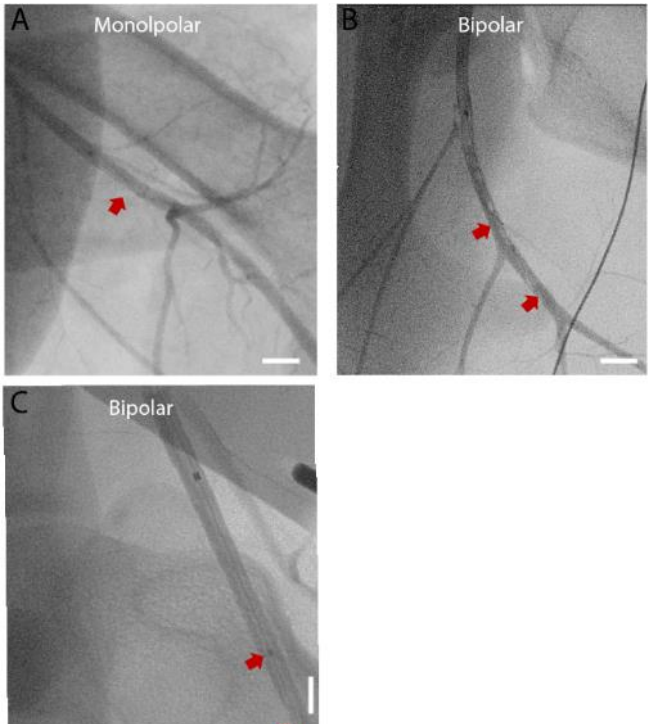

Figure 8. Endovascular treatment of the femoral artery. (A) A contrast-enhanced Angiogram image of the femoral artery following 400V pulses applied for 4min at 2Hz, displaying little or no constriction in the femoral artery in the monopolar configuration. Red arrow: electrode tip. (B) A contrast-enhanced angiogram image of the femoral artery following 400V pulses applied for 2min at 2Hz, displaying little or no constriction in the femoral artery in the bipolar configuration. Red arrows: electrodes. (C) A contrast-enhanced angiogram image of the femoral artery following 400V pulses applied for 4min at 2Hz, displaying little or no constriction in the femoral artery in the bipolar configuration. Red arrows: electrodes.

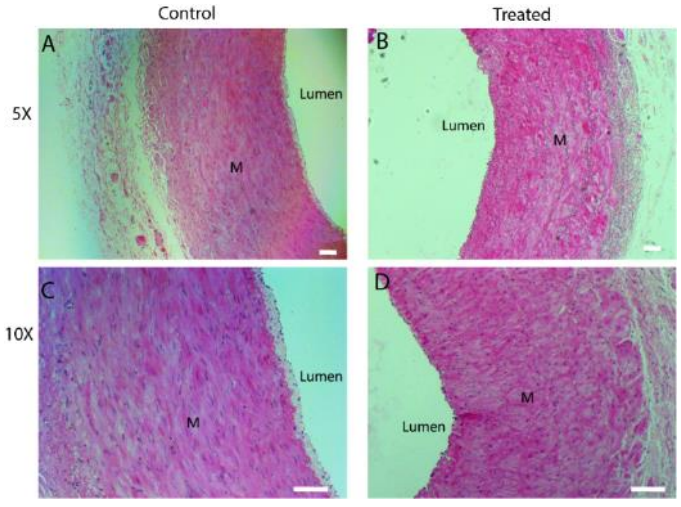

Figure 9. Immunohistology investigation of treatment safety. (A) &(C) hematoxylin and eosin (H&E) staining of a control femoral artery (A) 5x magnification and (C) 10x magnification. (B) & (D) hematoxylin and eosin (H&E) staining of a femoral artery following treatment (400V pulses, 1msec, administered for 1min at 2Hz). (B) 5x magnification and (D) 10x magnification. Scale bar - 50µm. M- Media

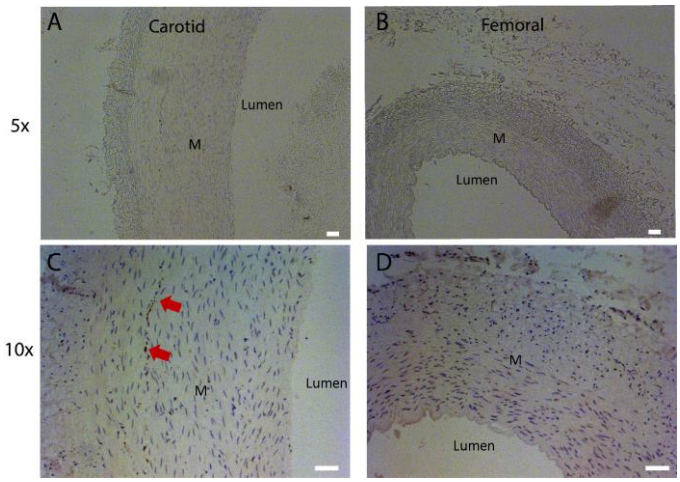

Figure 10. Immunohistology investigation of sympathetic system innervation. (A)&(C) The carotid artery processed for the sympathetic system marker Tyrosine Hydroxylase (A) 5x magnification. (C) 10x magnification revealing the sympathetic system nerve fibers (red arrows). (B)&(D) The femoral artery processed for the sympathetic system marker Tyrosine Hydroxylase. (B) 5x magnification and (D) 10x magnification revealing the lack of sympathetic system innervation of the femoral artery. Scale bar - 50µm. M-media

Interestingly, anti-Tyrosine hydroxylase staining revealed a high density of sympathetic nerve fibers in the carotid artery (Fig. 10a,c), whereas no staining was observed in the femoral artery (Fig. 10b,d), supporting our hypothesis of sympathetic nervous system innervation as a possible underlying mechanism for the endovascularly induced vasoconstriction.

IV. Discussion

Electrically induced vasoconstriction can be a valuable technique for hemorrhage control in cases where the widely used techniques are not applicable. Here, we have demonstrated robust vascular constriction of large arteries in response to endovascular application of a pulsed electric field. In contrast to previous approaches, based on external application[7], [26][27][8] of the electric field, the current approach provides an easy access to internal arteries, localization of the electric field to the arterial wall, and a negligible temperature rise. These capabilities can potentially enable better control of large artery constriction in cases of large cavities or junctional hemorrhages. Whereas previous studies using an external electrode focused on small arteries (500-800 µm)[8],[7] or solid organs[9], here we report for the first time, the successful application of pulsed electrical treatment on a large (8mm diameter) artery in a large animal, with a robust vasoconstriction response and a 7-fold decrease in bleeding from an arterial injury.

The concepts and methods introduced here can potentially provide new routes for controlling blood vessels, not only for traumatic injuries but also during elective vascular surgery. To date, hemostasis in vascular surgeries is achieved by exposing and mechanically clamping both the distal and proximal vascular ends, which is a time-consuming and technically

challenging procedure. However, these challenges can be potentially overcome through the introduced concept and application of electrical pulses with customized bipolar endovascular electrodes, which was shown here to induce two separate focal areas of constriction (Fig. 3b,d,f). It is worth noting that, as desired, following treatment a good recovery of the blood vessel diameter was observed with the time to return to baseline, depending on the applied pulse amplitude, similar to our previous reports in rats[7]. Small-size flexible electrodes can be introduced to almost every organ in the body and can thus be utilized for the treatment of bleeding or as an aid in hemostasis during surgery. Another potential advantage of the current approach is the induction of several constriction locations (e.g. Fig. 3f), compared with the commonly used micro-balloons which result in a single constriction site. An additional possible application of this concept is stimulation of vascular autonomic nerves for blood pressure and heart rate control (e.g. [28],[29]).

The bipolar configuration was slightly more efficient in inducing the desired vasoconstriction, compared with the remote ground monopolar configuration (Fig. 4). Further customization of the electrodes to a specific vessel dimension and geometry can aid in enhancing treatment efficiency and safety (Fig. 2 and [23]). Despite the focused field, the pulsed application was accompanied by muscle contraction, which necessitated the administration of muscle relaxants for paralysis in cases where a high-amplitude current was applied. Future studies should aim at studying approaches for reducing the muscle contraction, such as different pulse shapes[30],[31].

The close proximity of the endovascular electrodes to the heat-conducting blood flow contributed to the negligible estimated temperature increase treatment even for blood flow as low as 1 percent. Notwithstanding the observed safety, when a complete blood flow occlusion is desired, treatment should be carefully planned and adjusted (by reducing pulse amplitude, pulse duration, repetition rate, and treatment duration), to reduce the risk of a potentially harmful increase in temperature. It should be mentioned, that in the current model we assumed that the electrode is located in the center of the artery, as is predicted by the symmetrical forces applied by the blood flow. In the case of a radial deviation, the electric field and heat produced by the electrodes will increase on the close arterial edge and decrease on the far edge.

Finally, in previous studies, it was suggested that the mechanism underlying the induced vasoconstriction combines the direct effect of the electrical pulse on smooth muscle, and an indirect effect via activating sympathetic nerves[10]. In line with this hypothesis, we observed that the carotid artery, which is densely innervated by sympathetic system nerve fibers in the adventitia (Fig. 10 and [11],[32]) was more amenable to the applied treatment, demonstrating a robust response, compared with the less innervated femoral artery, which displayed little to no vasoconstriction. It is worth noting that in previous reports we observed robust constriction of the femoral artery of the rat [7], [8], which is highly innervated by sympathetic nerves[11],[32], compared with the sparse innervation of the sheep femoral artery (Fig. 10). Thus, the current study shows that sympathetic innervation plays a major role in the mechanism underlying electrical induced vasoconstriction. More studies are needed to further understand and explore the large variation obtained in the response of different blood vessels to short electrical pulse treatment.

Future studies are needed for exploring the potential of direct sympathetic nerve fibers stimulation (e.g. in the carotid bulb). This approach, however, will necessitate exploratory surgical effort and will probably cause a diffuse rather than localized response obtained with the current endovascular approach. Using a neural and muscular response prediction model can further enhance future research aimed at the reduction of the injected current, which is important for the reduction of involuntary muscle contraction and lowering the risk of cardiac arrhythmias, both are currently of main concerns for translating this approach to the clinic. Of another interest is to study potential chronic and late effects of electrical stimulation on the blood vessel wall, as the current research was limited to studying the acute stage pathological changes.

V. Conclusion

The reported results establish the concept of endovascular pulsed electrical treatment and present a first proof of concept of the feasibility and safety of this method, thus paving the way for a novel tool for vessel constriction for hemorrhage control as well as other applications. More research is needed to explore the potential of this technology in clinical applications.

Acknowledgment

The authors would like to thank Dr. Zohar Gavish at Gavish Research Services for performing the histological work; Dr. Udi Willenz and the Pre-clinical R&D Unit team in Yitzhak Shamir Medical Center for performing the angiography; and Mr. Yoav Chemla for acquiring the histological images

References

[1] CDC, “CDC - Injury - WISQARS (Web-based Injury Statistics Query and Reporting System),” *Injury prevention and control :Data and statistics*, 2004. [Online]. Available: http://www.cdc.gov/injury/wisqars/index.html.

[2] G. E. Katzenell U, Ash N, Tapia AL, Campino GA, “Analysis of the causes of death of casualties in field military setting.,” *Mil Med.*, vol. 177, no. 9, pp. 1065–8, 2012.

[3] B. L. Kragh JF Jr, Murphy C, Dubick MA, Baer DG, Johnson J, “New tourniquet device concepts for battlefield hemorrhage control.,” *US Army Med Dep J.*, 2011.

[4] J. F. Kragh *et al.*, “Battle casualty survival with emergency tourniquet use to stop limb bleeding,” *J.*

Emerg. Med., vol. 41, no. 6, pp. 590–597, 2011.

[5] H. J. Kragh JF Jr, Walters TJ, Baer DG, Fox CJ, Wade CE, Salinas J, "Practical use of emergency tourniquets to stop bleeding in major limb trauma.," *J Trauma.*, vol. 64, no. 2, pp. S38-49, 2008.

[6] N. A. and G. H. Yuval Rana, Eran Hadada, Saleh Dahera, Ori Ganora, Jonathan Kohna, Yana Yegorova, Carmi Bartala, "QuikClot Combat Gauze Use for Hemorrhage Control in Military Trauma: January 2009 Israel Defense Force Experience in the Gaza Strip—A Preliminary Report of 14 Cases," *Prehosp. Disaster Med*, vol. 25, no. 6, pp. 584–8, 2010.

[7] Y. Mandel *et al.*, "Vasoconstriction by Electrical Stimulation: New Approach to Control of Non-Compressible Hemorrhage.," *Sci. Rep.*, vol. 3, p. 2111, 2013.

[8] M. R. Brinton, Y. Mandel, R. Dalal, and D. Palanker, "Miniature electrical stimulator for hemorrhage control," *IEEE Trans. Biomed. Eng.*, vol. 61, no. 6, pp. 1765–1771, 2014.

[9] Y. Mandel *et al.*, "Hemorrhage Control of Liver Injury by Short Electrical Pulses," *PLoS One*, vol. 8, no. 1, 2013.

[10] M. Brinton, Y. Mandel, I. Schachar, and D. Palanker, "Mechanisms of electrical vasoconstriction.," *J. Neuroeng. Rehabil.*, vol. 15, no. 1, p. 43, May 2018.

[11] G. Gabella, "Complex Structure of the Common Carotid Artery of Sheep," *Anat. Rec.*, vol. 243, pp. 376–383, 1995.

[12] "Dielectric Properties of Body Tissues: Home page." [Online]. Available: http://niremf.ifac.cnr.it/tissprop/. [Accessed: 13-Jun-2018].

[13] S. Gabriel, R. W. Lau, and C. Gabriel, "The dielectric properties of biological tissues: III. Parametric models for the dielectric spectrum of tissues," *Phys. Med. Biol.*, 1996.

[14] A. Ivorra, B. Al-Sakere, B. Rubinsky, and L. M. Mir, "In vivo electrical conductivity measurements during and after tumor electroporation: conductivity changes reflect the treatment outcome.," *Phys. Med. Biol.*, vol. 54, no. 19, pp. 5949–5963, 2009.

[15] L. Silve, R. Qasrawi, and A. Ivorra, "Incorporation of the Blood Vessel Wall into Electroporation Simulations," Springer, Singapore, 2016, pp. 223–227.

[16] B. Al-Sakere *et al.*, "Tumor ablation with irreversible electroporation," *PLoS One*, 2007.

[17] E. H. Liu, G. M. Saidel, and H. Harasaki, "Model analysis of tissue responses to transient and chronic heating.," *Ann. Biomed. Eng.*, vol. 31, no. 8, pp. 1007–14, Sep. 2003.

[18] P. A. Hasgall *et al.*, "IT'IS Database for Thermal and Electromagnetic Parameters of Biological Tissues." 01-Jan-2012.

[19] Z.-S. Deng and J. Liu, "Blood perfusion-based model for characterizing the temperature fluctuation in living tissues," *Phys. A Stat. Mech. its Appl.*, vol. 300, no. 3–4, pp. 521–530, Nov. 2001.

[20] A. T. Riordan, C. Gamache, and S. W. Fosko, "Electrosurgery and cardiac devices.," *J. Am. Acad. Dermatol.*, vol. 37, no. 2 Pt 1, pp. 250–5, Aug. 1997.

[21] Y. C. Jou, M. C. Cheng, J. H. Sheen, C. Te Lin, and P. C. Chen, "Electrocauterization of bleeding points for percutaneous nephrolithotomy," *Urology*, vol. 64, no. 3, pp. 443–447, 2004.

[22] M. A. American Society for Dermatologic Surgery., C. K. Bichakjian, F. Pelosi, D. Blum, T. M. Johnson, and P. M. Farrehi, *Dermatologic surgery*. Elsevier Science Pub. Co, 2011.

[23] N. Kezurer, N. Farah, and Y. Mandel, "Endovascular Electrodes for Electrical Stimulation of Blood Vessels for Vasoconstriction – a Finite Element Simulation Study," *Sci. Rep.*, vol. 6, p. 31507, Aug. 2016.

[24] H. Pennes, "Analysis of tissue and arterial blood temperatures in the resting human forearm," *J. Appl. Physiol.*, pp. 5–34, 1948.

[25] R. Agah, J. A. Pearce, A. J. Welch, and M. Motamedi, "Rate process model for arterial tissue thermal damage: implications on vessel photocoagulation.," *Lasers Surg. Med.*, vol. 15, no. 2, pp. 176–84, 1994.

[26] D. Palanker, A. Vankov, Y. Freyvert, and P. Huie, "Pulsed electrical stimulation for control of vasculature: Temporary vasoconstriction and permanent thrombosis," *Bioelectromagnetics*, vol. 29, no. 2, pp. 100–107, 2008.

[27] G. Malki, O. Barnea, and Y. Mandel, "Hemorrhage Control by Short Electrical Pulses In Vivo Experiments," in *Biostec 2013 Proceedings of the International Conference on Biomedical Electronics and Devices*, 2012, pp. 103–107.

[28] D. T. T. Plachta *et al.*, "Blood pressure control with selective vagal nerve stimulation and minimal side effects," *J. Neural Eng.*, vol. 11, no. 3, p. 036011, Jun. 2014.

[29] J. Sun *et al.*, "Electrical Stimulation of Vascular Autonomic Nerves: Effects on Heart Rate, Blood Pressure, and Arrhythmias."

[30] Q. Castellví, B. Mercadal, X. Moll, D. Fondevila, A. Andaluz, and A. Ivorra, "Avoiding neuromuscular stimulation in liver irreversible electroporation using radiofrequency electric fields," *Phys. Med. Biol.*, vol. 63, no. 3, p. 035027, Jan. 2018.

[31] C. B. Arena *et al.*, "High-frequency irreversible electroporation (H-FIRE) for non-thermal ablation without muscle contraction.," *Biomed. Eng. Online*, vol. 10, p. 102, Nov. 2011.

[32] W. R. Keatinge and C. Torrie, "Action of sympathetic nerves of inner and outer muscle of sheep carotid artery, and effect of pressure on nerve distribution.," *J. Physiol.*, vol. 257, no. 3, pp. 699–712, Jun. 1976.